Istituto Nazionale di Fisica Nucleare
Sezione di Milano

INFN/AE-75/5
24 Aprile 1975

F. Palombo and M. Tarantini: STUDY ON THE PRECISION AND EFFICIENCY PECULIARITIES IN THE RECONSTRUCTION OF COHERENTLY PRODUCED EVENTS TAKEN BY M.I.S. CHAMBER OF DUBNA-SERPUKHOV. -

INTRODUCTION. -

The present work collects the analysis and calculations made to evaluate the efficiencies of pattern recognition end geometry reconstruction and the measure resolution for an experiment of elementary particles at high energy, which the Spark-Chamber-Group of Milan is now running at the Serpukhov 70-GeV accelerator, in collaboration with a group of physicists of the Dubna Nuclear Laboratory.

In the following chapters we describe two kinds of analyses:

- the first one gives the dependence of the errors with which invariant mass and 4-momentum transfer measurements will be performed from instrumental and measurements ones. The analysis is applied to events of two kinds, Montecarlo events and events extrapolated from a lower energy experiment;
- the second analysis, complementary to the first one, gives the efficiencies of the reconstruction chain (pattern recognition and geometry), starting from the extrapolated events.

In both cases the M.I.S. apparatus is simulated.

Preliminary, we briefly describe the physics of the experiment and the experimental set-up for a better understanding of the present work.

1. - SHORT DESCRIPTION OF THE EXPERIMENT. -

The reactions we shall study are of coherent production of bosonic systems on nucleus, precisely:

(1) π^- Nucleus $\longrightarrow 3\pi$ Nucleus

(2) π^- Nucleus $\longrightarrow 5\pi$ Nucleus

(3) π^- Nucleus $\longrightarrow K^- \pi^+ \pi^-$ Nucleus

Eight different nuclei (from Be to Pb) will be used, with 40 GeV maximum energy of the incident particle.

The events (1), (2), (3) will be analysed in a great spark chamber, with a magnetic field of about 17 KiloGauss. This chamber is constitued by 50 units, grouped two by two, as showed in Fig. 1 (only one unit for each pair is drawn).

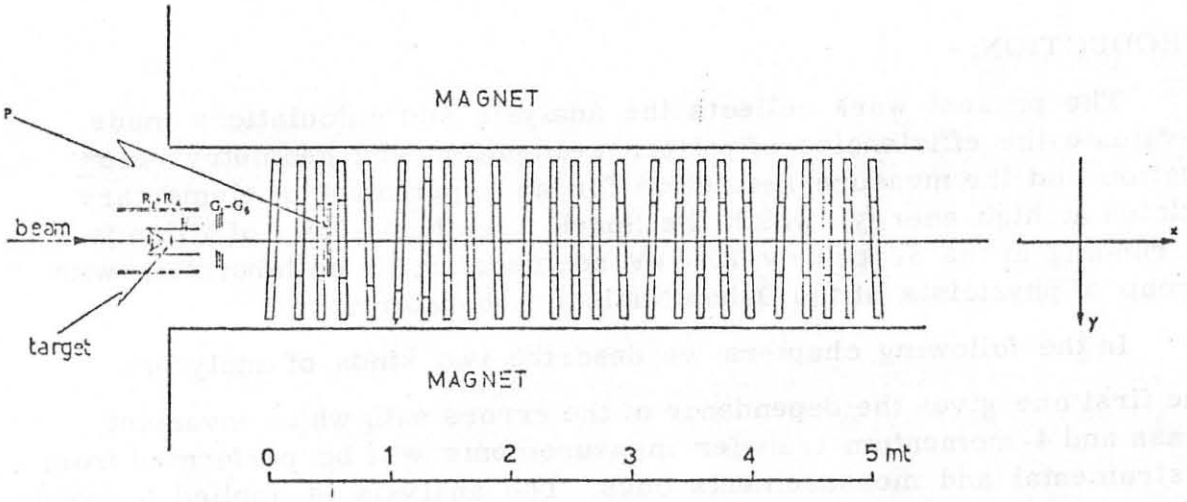

FIG. 1

Each plate of the units has a central window of Al (diameter 60 cm, thickness 57 μ), surrounded by an external thickness of 3 mm Al. One copper diaphragm per unit (8 mm thick) is placed in the region around the central window, to detect γ originated from π emitted at intermediate angles.

In the units from the 7^{th} to the 14^{th}, the central windows have been widened to get a high efficiency also for angles near to the maximum acceptance value (for systems of particles produced with high invariant masses).

The beam is defined by a series of scintillator counters and two Cerenkovs; ten wire spark chambers along the beam will allow an off--line reconstruction of the incident particles arrived in the 200-500 nsec interval before each trigger, between which there is the interacting one.

Around the target we find a cylindrical (F_1) and a conic (F_2) counter, a system of lead scintillator sandwiches R_1-R_4, to anticoincide emitted at great angles or protons incoherently produced.

Behind this system there is a lead-scintillator sandwich (G_1-G_6), which defines an acceptance cone of $13^o 40'$ and a multiwire proportional chamber P, in order to count the number of prongs of the produced system and therefore to select events with multiplicity of fast charged particles greater than 3.

Finally, behind the spectrometer we have the beam killer counter K; the final trigger will be:

$$(B\bar{K})(\bar{F}_1 \bar{F}_2 \prod_i \bar{R}_i \prod_i \bar{G}_i)\ (P[n \geq 3])$$

where B denotes the total signal defining the beam.

The events are photographed by means of two stereoscopic cameras with the optical axes parallel to z-axis (direction of magnetic field) and symmetrical as to yz plane (see Figs. 2 and 3).

To cover the whole length of the spectrometer, ten mirrors two by two stereoscopically grouped will be used; therefore the optical system is equivalent to 2 x 5 stereoscopic virtual cameras, each couple covering about 1 meter of length.

For details on the experiment we refer to reference (5).

2. - INTRINSIC RESOLUTION OF THE SPARK CHAMBER. -

2.1. - Spatial resolution. -

The main contribution to the spatial resolution that is the precision we can obtain in reconstructing a point (a spark) in the chamber -- are the following:

i) the spark formation mechanism;

ii) the distorsion due to the optical apparatus (lenses, mirrors, etc), the quality of the film and the development process; moreover the pre

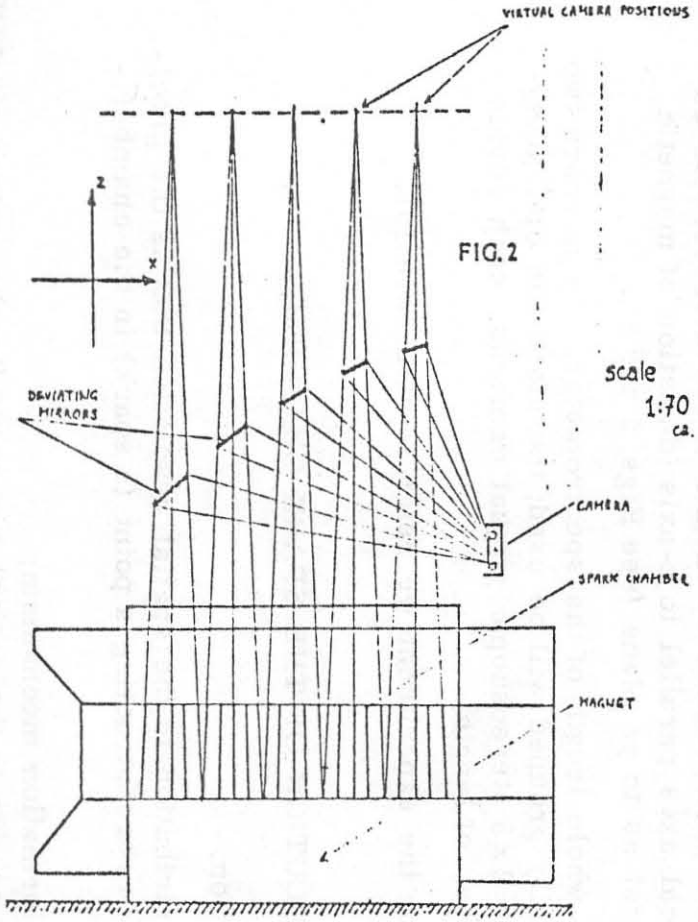
VIRTUAL CAMERA POSITIONS
z
x
FIG. 2
scale
1:70
ca.
DEVIATING MIRRORS
CAMERA
SPARK CHAMBER
MAGNET

FIG. 2

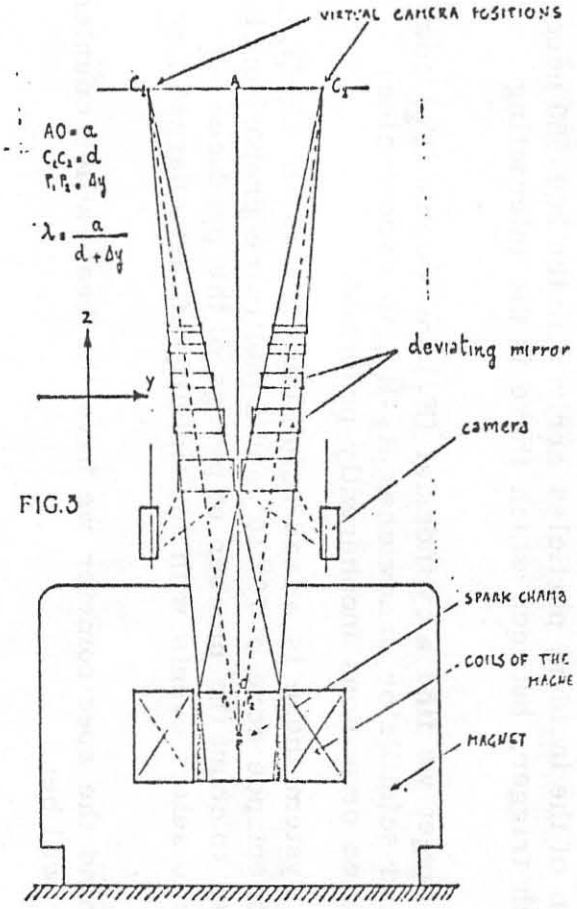
VIRTUAL CAMERA POSITIONS
C_1
A
C_2
AO = a
C_1C_2 = d
P_1P_2 = Δy
$\lambda = \frac{a}{d + \Delta y}$
z
y
FIG.3
deviating mirror
camera
SPARK CHAMB
COILS OF THE MAGNE
MAGNET

FIG. 3

cision of the apparatus for the automatic reading of the photographs(x). We shall denote all these errors with the term of "measure errors".

As regards point i), there is a systematic error due to the well knwon effects of drift and staggering of the single spark (see e.g. reference (1) p. 64-65 or ref. (2) app.). We only recall that this error is due to the combined action of the clearing field $\vec{E}$ and the magnetic field $\vec{B}$. The resulting deviation of the single spark position in the y-direction (parallel to the plates) is given by the formula:

$$\delta y = a + b \operatorname{tg} \phi \tag{4}$$

where ϕ is the angle between the track and the x-axis (normal to the plates) and a, b are two constants depending on $\vec{E}$, $\vec{B}$ and other parameters (as, for example, the delay-time; see ref. cit).

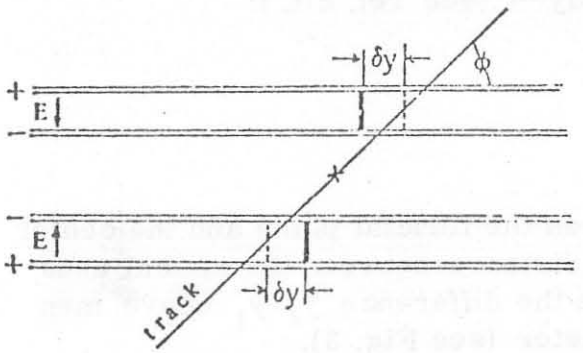

FIG. 4

As the sign of δy depends on the sign of E, we have a pratical method to correct automatically this systematic deviation: it is sufficient to give alternating signs to the clearing field in two near subsequant gaps (see Fig. 4) and to take the mean y-coordinate corresponding to the appropriate x-position.

Let's suppose to have corrected the systematic errors; it will remain an error due onlt to the random spark fluctuation in space: we'ill assume reasonably that:

$$\sigma_{y\,sp} = \sigma_{z\,sp} \tag{5}$$

The measure errors $\sigma_{y\,meas}$, $\sigma_{z\,meas}$ obviously cannot be evaluated separately from $\sigma_{y\,sp}$, $\sigma_{z\,sp}$; the only error we can evaluate experimentally is the total one, to which $\sigma_{y\,meas}$ and $\sigma_{y\,sp}$ contribute.

So we can write for the total y-error:

$$\sigma_y = \sqrt{\sigma_{y\,sp}^{\,2} + \frac{1}{2}\,\sigma_{y\,meas}^{\,2}} \tag{6}$$

(x) - The "Mark II HPD" of the CNAF of Bologna will be used in the present experiment.

(the factor 1/2 taking into account that there are two indipendent measurements of the same spark in the two wiews - see ref. (1) p. 67).

For the z-error we have similarly:

$$\sigma_z = \sqrt{\sigma^2_{z\,sp} + \sigma^2_{z\,meas}} \tag{7}$$

The z-co-ordinate is calculated by means of the difference $y_2 - y_1$ of the y in the two wiews (ref. (3), p. 53-54):

$$z = \lambda (y_2 - y_1) \tag{8}$$

λ is the stereoscopic factor of the optical system, depending on the geometry of the cameras; it is given by(x) (see ref. cit.):

$$\lambda = \frac{a}{d + \Delta y} \tag{9}$$

In this formula a is the distance between the fiducial plane and the center of the photographic cameras; d is the distance between the optical axes of the stereoscopic cameras and Δy is the difference $y_2 - y_1$ above mentioned, for the center of the spectrometer (see Fig. 3).

For example, in the "CERN Little Omega" chamber[1] it has been found $\lambda = 4.75$, whereas for the M.I.S. spectrometer we have estimated $\lambda \simeq 3.3$.

From (8), assuming equal measurements errors for y_1, y_2, we have:

$$\sigma^2_{z\,meas} = 2\,\lambda^2\,\sigma^2_{y\,meas} \tag{10}$$

and then, from (5) and (7):

$$\sigma_z = \sqrt{\sigma^2_{y\,sp} + 2\,\lambda^2\,\sigma^2_{y\,meas}} \tag{11}$$

With the quoted values of λ, in the (11) $\sigma_{y\,sp}$ becomes negligible as to $2\,\lambda^2\,\sigma^2_{y\,meas}$, so that:

(*) - This simple formula is valid in absence of refractive elements between the spectrometer and the lenses.

(12) $$\sigma_z \simeq \sqrt{2}\ \lambda\ \sigma_{y\,meas}$$

Therefore, measuring experimentally σ_z, we can evaluate $\sigma_{y\,meas}$; subsequently, by means of a measurement of σ_y, from (6) we can find $\sigma_{y\,sp}$.

σ_y is determined from the differences between measured and fitted spark coordinates.

We must notice that σ_y, σ_z depend on the azimuthal angle ϕ which the track forms with x-axis (normal to the plates). This has been found experimentally at CERN[1,2]:

(13) $$\sigma_y = 0.019 + 0.17\ \phi^2 \ \text{(cm)}$$

(14) $$\sigma_z = 0.06 + 0.22\ \phi^2 \ \text{(cm)}$$

Remembering that ϕ is very little in our events, we can concentrate our attention in the first term of σ_y. The other free parameters are the errors on P, λ, ϕ for the incident particle, that is $\Delta P/P$, $\Delta\lambda$, $\Delta\phi$. Finally the value σ_z can be obtained from (12) with the appropriate value of λ stereoscopic factor for M.I.S. spectrometer.

2.2.- Errors on the particle momenta due to the spatial resolution.-

The errors on the co-ordinates $(1/\varrho, \lambda, \phi)$ of a particle (which characterize its momentum), simply propagate from the errors σ_y, σ_z.

Here we only give the final results in form of error matrix on $(1/\varrho, \lambda, \phi)$ (for details see ref. (3), p. 45-48):

(18) $$\begin{bmatrix} \left(\frac{8\,\sigma_s}{L^2\cos^2\lambda}\right)^2 & 0 & -32\,\frac{\sigma_s\,\sigma_z}{L^3\cos^3\lambda} \\ 0 & \left(\frac{4\,\sigma_z}{L\cos\lambda}\right)^2 & 0 \\ -32\,\frac{\sigma_s\,\sigma_z}{L^3\cos^3\lambda} & 0 & \left(\frac{4\,\sigma_s}{L\cos\lambda}\right)^2 \end{bmatrix}$$

where σ_s is the error on sagitta of the track projected in the xy-plane and it is given by[4]:

(19) $$\sigma_s = 3.5\,\frac{\sigma_y\,\overline{(\phi^2)}}{\sqrt{N}}$$

(N is the number of measurable sparks). In (18) L denotes the length of measurable track.

2.3. - Errors on the particle momenta due to the multiple scattering in the chamber. -

These errors, independent from the previous ones, will be added quadratically to the measure ones to give the total errors on the momentum.

The matrix errors on $(1/\varrho\ ,\ \lambda\ ,\ \phi)$ is (ref. (3), p. 49-51):

$$(20) \qquad \begin{bmatrix} \frac{4}{3} & -\frac{K}{L\cos^4\lambda} & 0 & -\frac{K}{6\cos^3\lambda} \\ 0 & & \frac{KL}{3} & 0 \\ -\frac{K}{6\cos^3\lambda} & & 0 & \frac{KL}{6\cos^2\lambda} \end{bmatrix}$$

where:

$$K = \frac{1}{2}\,\frac{C}{p\beta} \quad \text{with } C = 0.021/\sqrt{L_o}$$

L_o = radiation length of the chamber (in cm)

p = particle momentum (in GeV/c).

2.4. - Simulation program. -

The program used to evaluate the experimental errors on $M_{3\pi}$ and 4-momentum transfer to the nucleus (in reactions (1), (2), (3)), simulates the experimental apparatus as described in the flow diagram of Fig. 5(x). For details see ref. (3), p. 58-75.

As fas as the input events are concerned, two kinds have been used:

(x) - This program is a modified and improved version (for M.I.S. apparatus) of a program kindly given us at CERN from L. Mandelli and adapted for the Univac Computer from M. Fiocca.

i) events entirely simulated with Montecarlo method.

ii) events transformed at the required energy (40 GeV) from events of a previous experience at lower energy (15 GeV). These events have the same mass - distribution of the 15-GeV ones, but they are more forward peaked, because in the previous experiment the events were already cut with an acceptance cone of 22^{o}; this corresponds, at 40 GeV, to an acceptance cone of about 8^{o}.

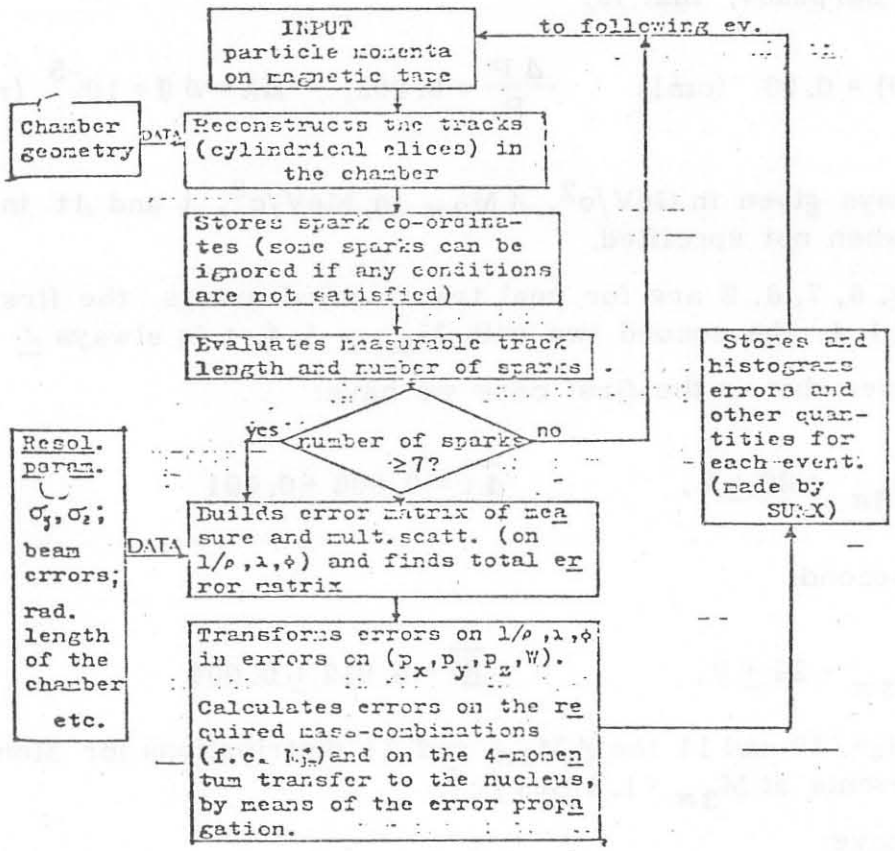

FIG. 5 - Flow-diagram of the program.

N.B. - In this program we don't care about pattern recognition problem, but the only condition in order that the track is reconstructed is that it has seven sparks at least. On the contrary, in chapter 3 the pattern recognition technique - as it will be used in the real events - is completely developed.

2.4. - Results of the program. -

We have performed the analysis with different groups of experimental parameters, that is σ_y, $\Delta P/P$, $\Delta \lambda$, $\Delta \phi$. The results on the real

transformed events are identical to those obtained on Montecarlo generated events at the same produced invariant mass $M_{3\pi}$. We have made the distributions of the error $\Delta M_{3\pi}$ on the produced mass $M_{3\pi}$ and of the error Δt on the tetra-momentum transfer at different mass and with different values for σ_y, $\Delta P/P$, $\Delta\lambda$, $\Delta\phi$.

We show now same distributions of the errors on $M_{3\pi}$ and t for parameters' values which seem to be at present the best for M.I.S. chamber of Serpukov, that is:

$$\sigma_y(\phi = 0) = 0.03 \quad (\text{cm}), \qquad \frac{\Delta P}{P} = 0.003, \qquad \Delta\lambda = \Delta\phi = 10^{-5} \quad (\text{rad})$$

$M_{3\pi}$ is always given in GeV/c^2, $\Delta M_{3\pi}$ in MeV/c^2, t and Δt in $(GeV/c)^2$, when not specified.

Figs. 6, 7, 8, 9 are for real transformed events, the first two with $M_{3\pi} < 1.4$, the second two with $M_{3\pi} \geq 1.4$. t is always ≤ 0.2.

We see that in the first case we have:

$$\overline{\Delta M}_{3\pi} = 20 \pm 7, \qquad \overline{\Delta t} = 0.006 \pm 0.001$$

In the the second:

$$\overline{\Delta M}_{3\pi} = 24 \pm 9, \qquad \overline{\Delta t} = 0.012 \pm 0.004$$

In Figs. 10 and 11 the $\Delta M_{3\pi}$ and Δt distributions for Montecarlo generated events at $M_{3\pi} = 1.2\ GeV/c^2$.

We have:

$$\overline{\Delta M}_{3} = 20 \pm 8, \qquad \overline{\Delta t} = 0.005 \pm 0.0004$$

We give the results for, other mass values:

$M_{3\pi} = 1.6$ $\quad \overline{\Delta M}_{3\pi} = 23.0 \pm 10$ $\quad \Delta t = 0.010 \pm 0.001$

$M_{3\pi} = 2.2$ $\quad \overline{\Delta M}_{3\pi} = 29 \pm 10$ $\quad \Delta t = 0.02 \pm 0.004$

$M_{3\pi} = 3.0$ $\quad \overline{\Delta M}_{3} = 41 \pm 16$ $\quad \Delta t = 0.044 \pm 0.013$

We notice that the best percentual error, ($\overline{\Delta M}/M \cdot 100$), is 1.3% and that we obtain this value around $M_{3\pi} = 2.2$ GeV/c^2.

From the comparison of all distributions we can infer that (see Table I and II):

1) The mean error $\Delta M_{3\pi}$ depends mainly on σ_y. Increasing σ_y of 0.01, $\Delta M_{3\pi}$ increases of about 5 MeV/c^2 at 1.2 GeV/c^2 and about 8 MeV/c^2 at 3 GeV/c^2, that is a variation of 20 - 25%.

2) The mean error $\overline{\Delta t}$ does not depend on $\Delta\lambda$ and $\Delta\phi$ for $\Delta\lambda$ and $\Delta\phi$ less than 1 mrad.

$\overline{\Delta t}$ depends slowly on $\Delta P/P$; for instance if $\Delta P/P$ goes from 10^{-6} to 0.003, $\overline{\Delta t}$ changes from 0.005 to 0.007. We remember that at Serpukov the value 0.003 for $\Delta P/P$ is the error on the beam available a priori from the beam design and that the use of wire spark chambers along the beam can reduce this error.

The mean error $\overline{\Delta t}$ depends on σ_y in such a way that if σ_y increases of 0.01, $\overline{\Delta t}$ increases of 0.001 at 1.2 GeV/c^2 (20%) and of 0.005 at 3 GeV/c^2 (10%).

We have seen also what changes if we take events with magnetic field equal to 12 KG (previous value 17 KG) at the same values of the other parameters.

$\overline{\Delta M_3}$ improves of about 3 MeV/c^2 at low mass ($M_{3\pi} < 1.6$ GeV/c^2) and increases of about 3 MeV/c^2 around $M_{3\pi} = 3$ GeV/c^2.

$\overline{\Delta t}$ increases of about 20% and 10% around 1.2 GeV/c^2 and 3 GeV/c^2 respectively.

As we'll see later the pattern recognition efficiency improves of 1% (this efficiency improvement is greater for 5 prongs events of course). With the set of parameters seen above and H = 12 KG (Montecarlo events) we have:

$M_{3\pi} = 1.2$ $\quad \overline{\Delta M}_{3\pi} = 17 \pm 5$ $\quad \overline{\Delta t} = 0.006 \pm 0.0009$

$M_{3\pi} = 3.0$ $\quad \overline{\Delta M}_{3\pi} = 45 \pm 20$ $\quad \overline{\Delta t} = 0.049 \pm 0.014$

3. - EFFICIENCY OF PATTERN RECOGNITION AND GEOMETRY RECONSTRUCTION PROGRAMS. -

3.1. - Description of the programs related with the simulation of events and their reconstruction. -

The D.D. division of CERN has set up a series of programs for

the off-line analysis of spark chamber events taken by the Omega(x), that is simulations of events, pattern recognition, momentum evaluation, event display programs and so on. These programs are strictly related with the basic features and the particular data acquisition of the Omega system.

We have modified and improved these programs in order to relate them with the particularities of M.I.S. chamber of Dubna-Serpukhov (see Chapter 1).

On account of space we can't give here an exhaustive description of these programs (see for this the Manuals edited by CERN) or all the modifications made on the official version (for which we refer to future papers).

We have used the programs SIMMEGA and PLUMEGA in order to simulate events produced by the M.I.S. chamber; the input of SIMMEGA are the kinematical data of the events (vertices, momenta and charge of particles etc). The program generates tracks in space with the proper curvature and lengths; PLUMEGA uses the output of SIMMEGA (co-ordinates of points on tracks in the chamber gaps), introduces some physical effects (staggering - (see p. 5), noise, efficiency etc.) and gives an output in a format suitable for input in the reconstruction program ROMEO.

ROMEO is the program for recognition and geometrical reconstruction of spark chamber events taken by the Omega. We have changed it in order to reconstruct events taken by the M.I.S. chamber of Serpukhov.

Shortly we can say that ROMEO consists of five modules: the first one reads control cards and calculates some secondary constants; the second is the fiducial mark one; the third is the pattern recognition one, which recognizes events and sends tracks to the fouth module, the geometry one, which computes the geometrical parameters of the tracks. The last module writes a summary of the analysed event.

3.2. - Simulated events. -

We have used for the simulation 100 events of coherent production on nucleus (Be), taken by a previous experiment at 15 GeV; they have been transformed at 40 GeV (see p. 9) and are 3-prongs events of find $\pi^- Be \rightarrow \pi$ Be.

Since we don't know with precision the whole magnetic field of the Dubna chamber, we have used the Omega one, increasing its dimension, not being substantial differences in shape and intensity.

The true magnetic field would give rise to some problems is

(x) - Omega is the big magnetic spark chamber working at CERN from 1970.

reconstruction of vertex: this point must be further on investigated.

For the staggering constants we have used the value 0,1 cm, while, in order to determine the spark position fluctuation, we have used the formula (see p.):

$$\sigma_{fluct} = 0.022 + 0.17\ \phi^2 \quad (cm)$$

We have introduced an efficiency of rivelation of correlated sparks (that is the same sparks missing in the two views) of 85%, as preliminarly measured by the physicists of Dubna in the first tests on the chamber.

Finally we have introduced background sparks in each wiew, in the set of 50 gaps of the chamber. We have simulated at random 15 sparks in the whole chamber: this doesn't rise to any problem in the reconstruction.

3.3. - Analysis of the results. -

3.3.1. - Efficiency in the reconstruction. -

Here we only consider the efficiency of pattern recognition and geometry, in the maximum volume of the chamber (therefore including the portions of plates with a greater thickness of copper and aluminium (see Chap. 1 and Fig. 1).

Here we have tested that multiple scattering affects little the reconstructed track parameters and errors (see after).

All the events are fitted by pattern recognition, that is we have an efficiency of track reconstruction of 100%. This happens since the pattern recognition module finds sparks enaugh to reconstruct the track- - also in the case of slow particles - in spite of simulated inefficiency. The simulated sparks background doesn't give rise to any problem, as already mentioned, because the sparks, being at random, are easily eliminated by the spark-following and complementation process; moreover the topology of our events is particularly simple.

We have made the same analysis with the Montecarlo events, obtaining:

$M_{3\pi} = 1.6$ P.R. Efficiency = 96%

$M_{3\pi} = 2.4$ P.R. Efficiency = 94%

In the first case using $H = 12^{KG}$ we have

P.R. Efficiency = 97%

(we notice an increasing of 1% of efficiency by lowering from 17 to 12 KG the field H).

3.3.2.- The geometry efficiency.-

As regards this point, we have an efficiency of 2 - 4% lower than the corresponding pattern recognition one; this efficiency is very sensible to the magnetic field around the target(x). If the magnetic field around the target is enough different from the one simulated by us (which is the Omega one), then the geometry efficiency could be very different. The extrapolation to the vertex is very good also because the spark error is very small.

The sparks simulated by us are, as above mentioned, single sparks, with 40-60 μ mean dimensions in the hypothesis that the HPD can find their center with an approximation of 3-4 μ . Obviously, if on the contrary the dimensions of the sparks were drastically larger, or if if there were frequently double or multiple sparks (in case of bad running of the chamber)(o), this analysis should be made again: in this case the effiencies and track parameters' errors should be greatly deteriorated.

In Fig. 12 and 13 we give the distributions of percentual errors on track momentum, separating the ones with $p > 0$ (charge +), from those ones with $p < 0$ (wharge -), with and without multiple scattering.

The distributions are gaussian inside the statistical errors: therefore no systematic errors seem to appear.

The multiple scattering spreads the distributions a little.

In Fig. 14 the distributions on $\phi_i - \phi_{out}$ are given: they are very peaked gaussian distributions, centered around the origin. The multiple scattering affects these errors very little.

In Fig. 15 the analogous deviation $\lambda_i - \lambda_{out}$ with and without multiple scattering, are given, for $\lambda_i > 0$ and $\lambda_i < 0$. We note a certain asymmetry in the histograms at very low λ . This is explained by the big errors in λ in the reconstruction program. All the same has been obtained with Monte Carlo generated events.

(x) - We recall that the distance of the target from the first gap is about 58 cm.

(o) - This effect is actually not simulated in our programs.

MASTER TESTS 4 .
XLOC 711

BITS	BINS	CAP.	LOST	NX	DELX	XLOW	XMEAN	XRMS	CONTENT	EXCL.	U-FLOW	O-FLOW
10	6	1023	0	100	.001	0.	.02024	.00745	862.		0.	0.

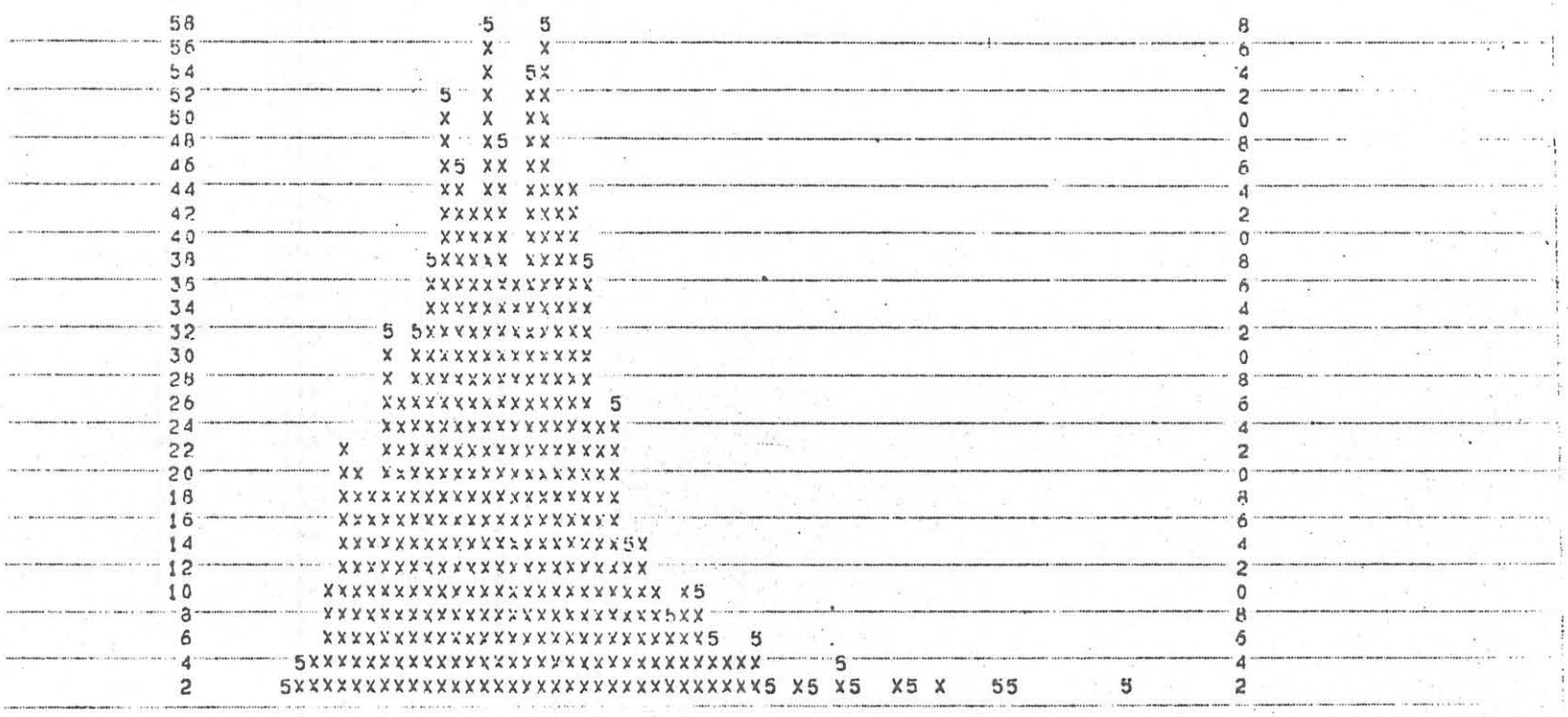

FIG. 6

TEST FOAL DATE 7n03[illegible]

BLS HGR 9 149 DISTRIBUZIONE DELTA T CON T MINORE DI ,02 E M* MINORE DI 1,4

MASTER TESTS 6 ,
XLOC 751

BITS	BINS	CAP,	LOST	NX	DELX	XLOW	XMEAN	XRMS	CONTENT	EXCL,	U-FLOW	O-FLOW
10	8	1023	0	100	,001	0,	,00582	,00156	620,		0,	0,

```
      155        6                5
      150        X                0
      145        X                5
      140        X                0
      135        X4               5
      130        8XX              0
      125        XXX              5
      120        XXX              0
      115        XXX              5
      110        XXX              0
      105        XXX              5
      100        XXX              0
       95        XXX              5
       90        XXX              0
       85        XXX              5
       80        XXX              0
       75        XXX4             5
       70        2XXXX            0
       65        XXXXX            5
       60        XXXXX            0
       55        XXXXX            5
       50        XXXXX            0
       45        XXXXX            5
       40        XXXXX8           0
       35        XXXXXX           5
       30        XXXXXX           0
       25        XXXXXX           5
       20        XXXXXX4          0
       15        XXXXXXX          5
       10        6XXXXXXX         0
        5        XXXXXXXX62       5

CON-      111
TENT     6253731
```

FIG. 7

BITS	BINS	CAP.	LOST	%X	DELX	XLOW	XMEAN	XRMS	CONTENT	EACL.	CAP.
10	6	1023	0	100	.001	0.	.02384	.00923	330.		

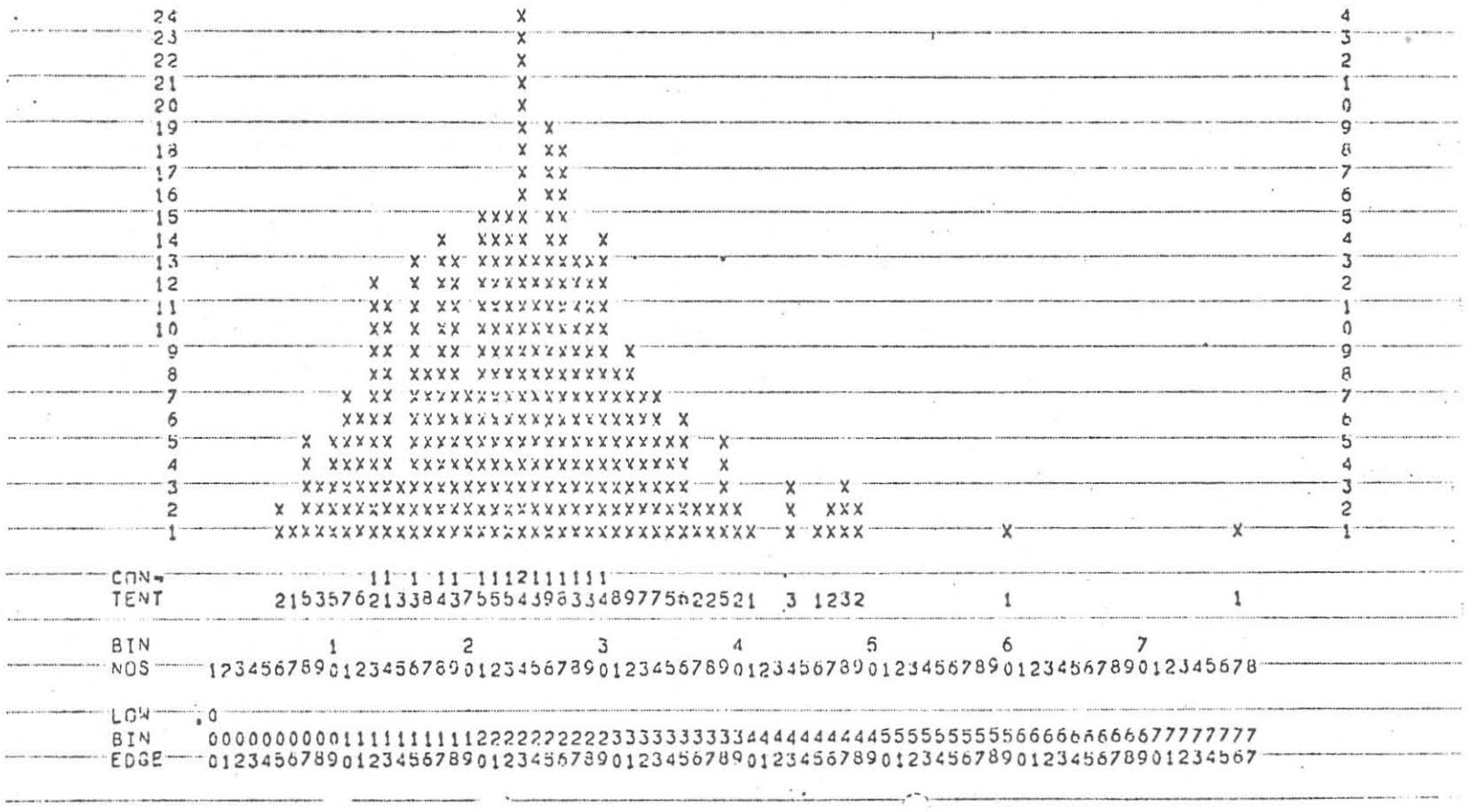

FIG. 8

```
PL5 HGR  10           1+10      1DISTRIBUZIONE DELTA T  CON T MINORE DI ,02 E M* MAGGIORE DI 1,2

MASTER TESTS    7 ,
XLOC  751

 BITS BINS  CAP,  LOST    NX    DELX     XLOW        XMEAN    XRMS  CONTENT  EXCL,  U-FLOW  O-FLOW
   10    6  1023     0   100    ,001       0,       ,01158  ,00372     187,              0,      0,

   28            X                          8
   27           XX                          7
   26           XX                          6
   25           XX                          5
   24          XXXX                         4
   23          XXXX                         3
   22          XXXX                         2
   21          XXXX                         1
   20          XXXX                         0
   19         XXXXX                         9
   18         XXXXX                         8
   17         XXXXXX                        7
   16         XXXXXX                        6
   15         XXXXXX                        5
   14         XXXXXX                        4
   13         XXXXXXX                       3
   12         XXXXXXX                       2
   11         XXXXXXX                       1
   10         XXXXXXXX                      0
    9         XXXXXXXX                      9
    8         XXXXXXXX                      8
    7         XXXXXXXX                      7
    6         XXXXXXXXX                     6
    5         XXXXXXXXX                     5
    4         XXXXXXXXX                     4
    3         XXXXXXXXXX   X   X            3
    2        XXXXXXXXXXXX  XX  X            2
    1        XXXXXXXXXXXXXXXX XX    X       1

CON-          12222111
TENT         2947847306321132 13    1

BIN               1         2         3
NOS    1234567890123456789012345678901

LOW    .0
BIN    0000000000111111111122222222223
```

FIG. 9

FO=L , M*=1.2

8L7 PROJ. 1 +1 DISTRIBUZIONE DELTA M* VS. M*

X = PROJECTION	LOST	MEAN	RMS	CONTENT	EXCL.	U-FLOW
	0	.019937	.0083	1266.		0.

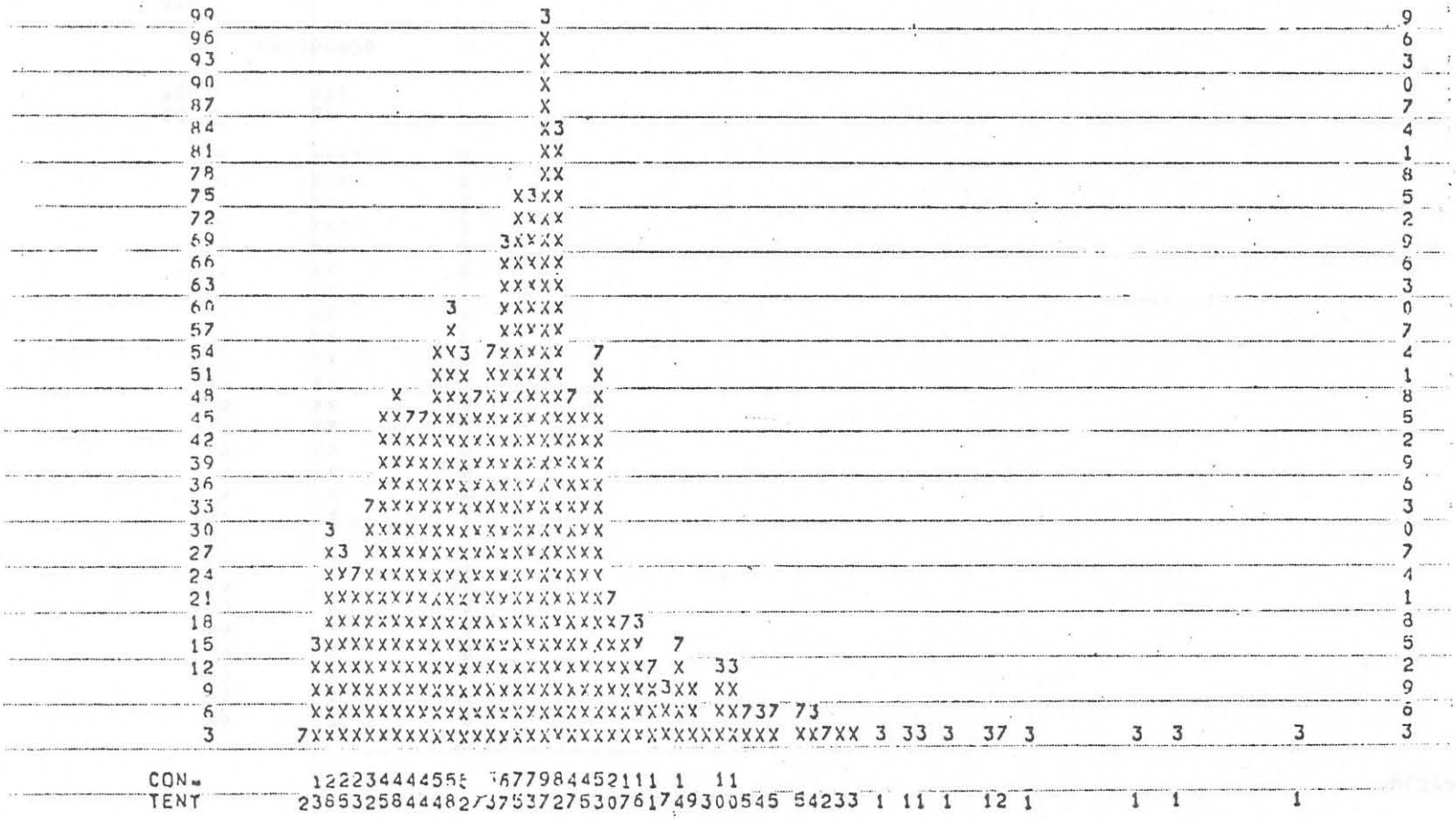

FIG. 10

```
GL7 PROJ.  2          1+2       'DISTRIBUZIONE DELTAT VS. T

                    X = PROJECTION    LOST     MEAN      RMS     CONTENT  EXCL.  U-FLOW  O-
                                         0  ,005267  ,000436     1266.                0.

                                                                              MULTIPLY

        78          7          8
        75          X          5
        72          X          2
        69          X          9
        66          X          6
        63          X          3
        60          X          0
        57          X          7
        54          X          4
        51          X          1
        48          X          8
        45          X          5
        42         2X          2
        39         XX          9
        36         XX          6
        33         XX          3
        30         XX          0
        27         XX          7
        24         XX          4
        21         XX          1
        18         XX          8
        15         XX          5
        12         XX3         2
         9         XXX         9
         6         XXX         6
         3         XXX1        3

   CON-           37
   TENT          979

                 .000050920

   BIN
   NOS     123456789

   LOW     .00
   BIN     012345678
   EDGE    0
```

FIG. 11

TABLE I

N. RUN	$\sigma_y(\phi=0)$ (cm)	$\Delta\lambda = \lambda\phi$ (rad)	$\frac{\Delta P}{P}$	$M_{3\pi} < 1.4$		$M_{3\pi} \geq 1.4$		$t \leq 0.02$		$M_{3\pi}$ 1.4 $t \leq 0.02$		$M_{3\pi} \geq 1.4$ $t \leq 0.02$	
				$\overline{\Delta M}_{3\pi}$	$\sigma_{\overline{\Delta M}_{3\pi}}$	$\overline{\Delta M}_3$	$\sigma_{\overline{\Delta M}_{3\pi}}$	$\overline{\Delta t}$	$\sigma_{\overline{\Delta t}}$	$\overline{\Delta t}$	$\sigma_{\overline{\Delta t}}$	$\overline{\Delta t}$	$\sigma_{\overline{\Delta t}}$
1	0.05	10^{-7}	10^{-6}	31	10	35	13	0.007	0.004	0.006	0.003	0.011	0.004
2	0.04	10^{-7}	10^{-6}	25	9	30	11	0.006	0.003	0.005	0.002	0.009	0.004
3	0.03	10^{-7}	10^{-6}	20	7	24	9	0.005	0.003	0.004	0.002	0.008	0.003
4	0.02	10^{-7}	0.003	15	6	18	7	0.004	0.002	0.003	0.001	0.006	0.003
5	0.03	10^{-7}	0.003	20	7	24	9	0.007	0.003	0.006	0.001	0.012	0.004
6	0.03	10^{-6}	0.003	20	7	24	9	0.007	0.003	0.006	0.001	0.011	0.004
7	0.03	10^{-5}	0.003	20	7	24	9	0.007	0.003	0.006	0.001	0.012	0.004
8	0.03	10^{-4}	0.003	20	7	24	9	0.007	0.003	0.006	0.001	0.012	0.004
9	0.03	10^{-3}	0.003	20	7	24	9	0.010	0.003	0.008	0.002	0.013	0.004
10	0.02	10^{-5}	0.003	15	6	18	7	0.006	0.003	0.005	0.001	0.010	0.003
111	0.04	10^{-5}	0.003	25	9	30	11	0.008	0.004	0.007	0.002	0.013	0.004
12	0.05	10^{-5}	0.003	31	10	35	13	0.009	0.004	0.008	0.002	0.014	0.005
13	0.0	10^{-5}	0.003	6	4	8	5	0.005	0.003	0.004	0.001	0.009	0.003
14	0.03	10^{-5}	0.003	17	6	22	8	0.008	0.005	0.006	0.002	0.014	0.008
15	0.05	10^{-5}	0.003	26	8	32	10	0.011	0.006	0.008	0.003	0.018	0.010

RUN 14 = RUN 7 + H = 12 (KG)

RUN 15 = RUN 12 + H = 12 (KG)

TABLE II

N. RUN	$\sigma_y(\phi=0)$ (cm)	$\Delta\lambda = \Delta\phi$ (rad)	$\frac{\Delta P}{P}$	$M_{3\pi}$	$\overline{\Delta M}_{3\pi}$	$\sigma\overline{\Delta M}_3$	$\overline{\Delta t}$	$\sigma\overline{\Delta t}$
1	0.05	10^{-7}	10^{-6}	1.2	30	11	0.004	0.0012
2	0.04	10^{-7}	10^{-6}	1.2	25	10	0.004	0.0009
3	0.03	10^{-7}	10^{-6}	1.2	20	8	0.003	0.0007
4	0.02	10^{-7}	0.003	1.2	15	7	0.002	0.0005
5	0.03	10^{-7}	0.003	1.2	20	8	0.005	0.0004
6	0.03	10^{-6}	0.003	1.2	20	8	0.005	0.0004
7	0.03	10^{-5}	0.003	1.2	20	8	0.005	0.0004
8	0.03	10^{-4}	0.003	1.2	20	9	0.005	0.0004
9	0.03	10^{-3}	0.003	1.2	20	9	0.005	0.0004
10	0.02	10^{-5}	0.003	1.2	15	7	0.005	0.0003
11	0.04	10^{-5}	0.003	1.2	25	10	0.006	0.0006
12	0.05	10^{-5}	0.003	1.2	30	11	0.006	0.0008
13	0.0	10^{-5}	0.003	1.2	5	4	0.005	0.0001
14	0.03	10^{-5}	0.003	1.6	23	10	0.010	0.0009
15	0.05	10^{-5}	0.003	1.6	35	14	0.012	0.0017
16	0.03	10^{-5}	0.003	2.2	29	10	0.020	0.004
17	0.05	10^{-5}	0.003	2.2	41	14	0.024	0.005
18	0.03	10^{-5}	0.003	3.0	41	16	0.044	0.013
19	0.05	10^{-5}	0.003	3.0	55	17	0.053	0.012
20	0.03	10^{-5}	0.003	1.2	20	5	0.006	0.0009
21	0.05	10^{-5}	0.003	1.2	26	8	0.007	0.0015
22	0.03	10^{-5}	0.003	3.0	45	20	0.049	0.014
23	0.05	10^{-5}	0.003	3.0	57	18	0.059	0.012

Run 20 = Run 7 + H = 12 (KG) Run 22 = Run 18 + H = 12 (KG)

Run 21 = Run 12 + H = 12 (KG) Run 23 = Run 18 + H = 12 (KG)

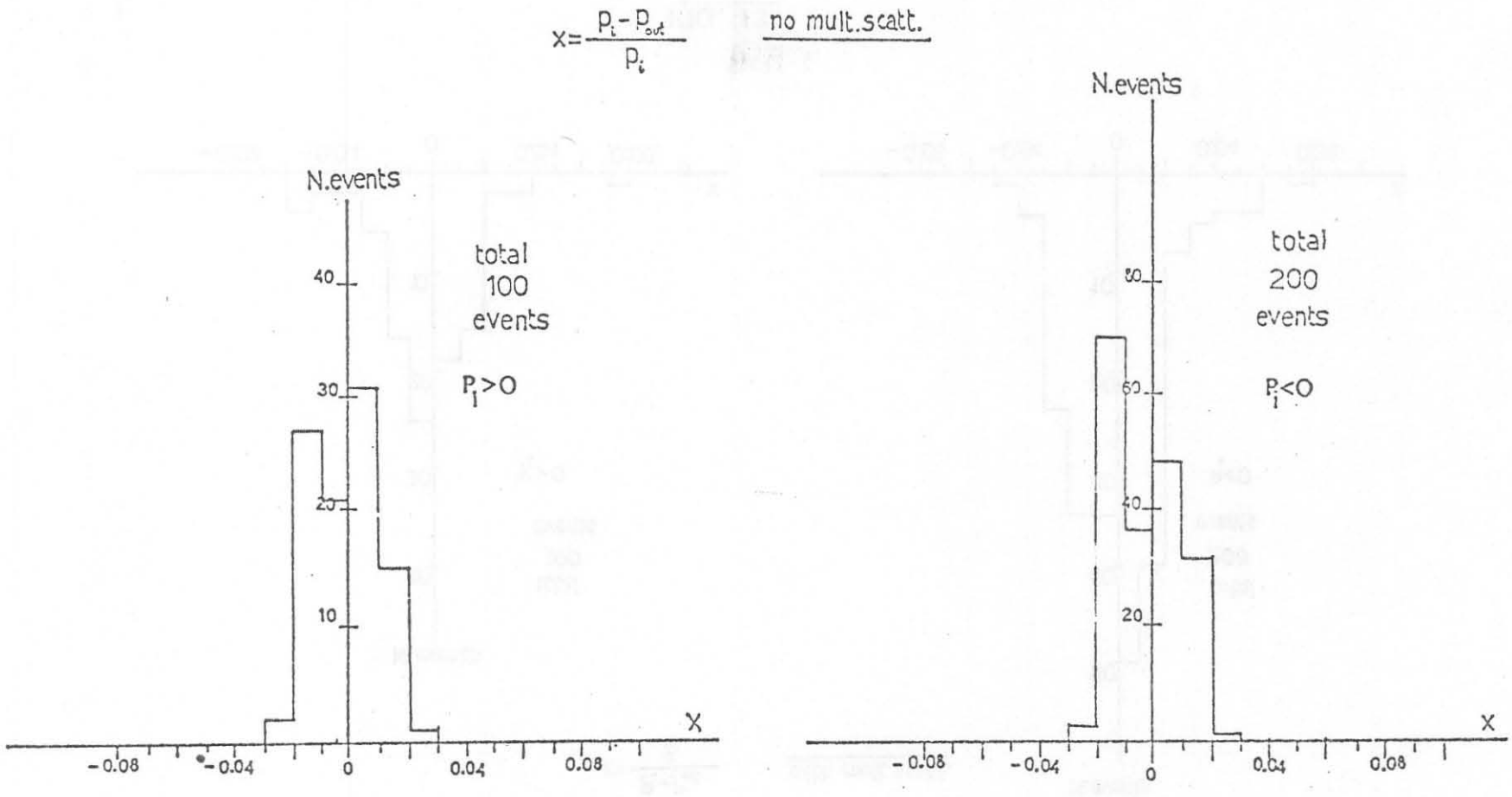
$x = \frac{P_i - P_{out}}{P_i}$
no mult.scatt.
N.events
total
100
events
$P_i > 0$
40
30
20
10
X
-0.08
-0.04
0
0.04
0.08
N.events
total
200
events
$P_i < 0$
80
60
40
20
X
-0.08
-0.04
0
0.04
0.08

FIG. 12

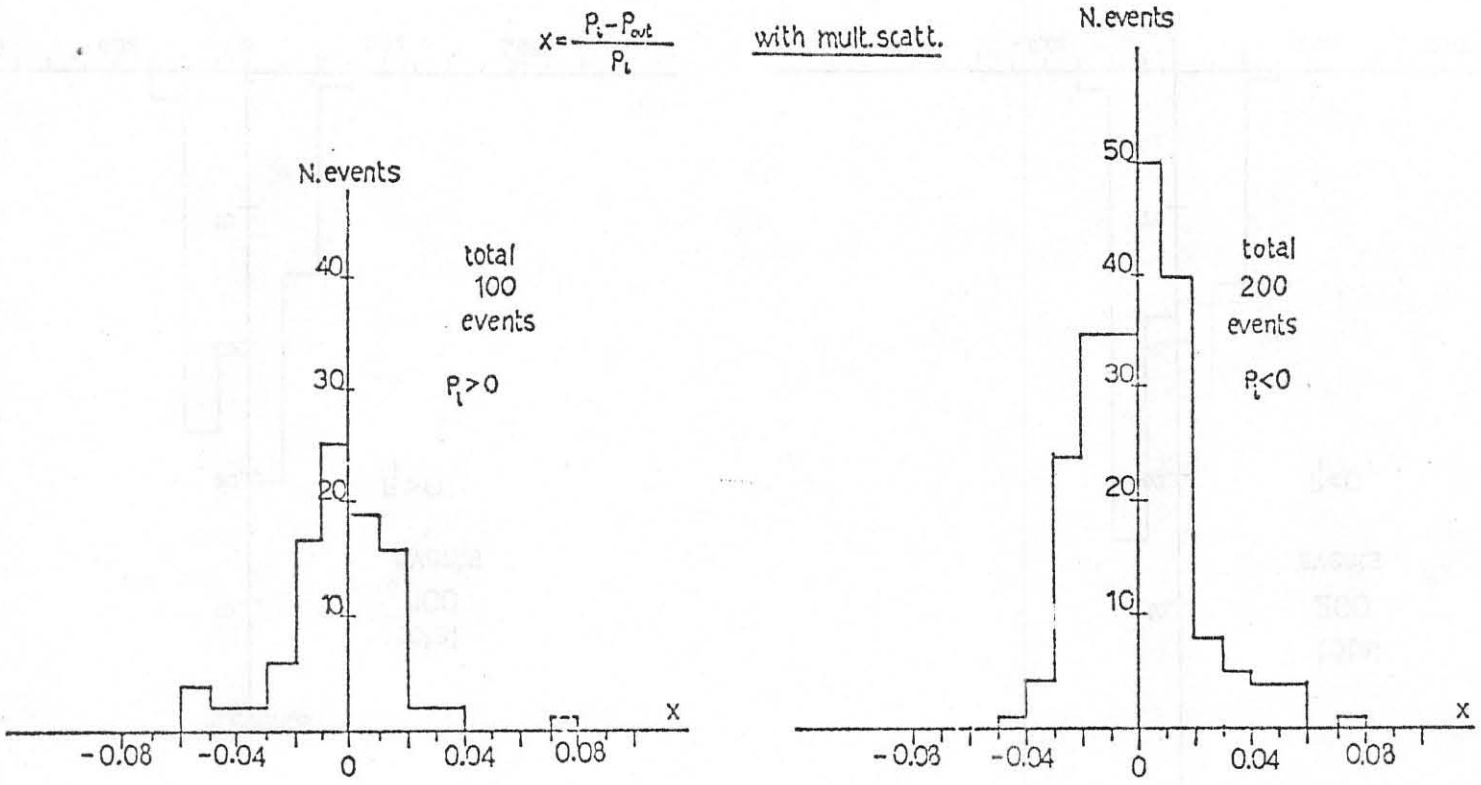
$x = \frac{P_t - P_{out}}{P_t}$
with mult.scatt.
N.events
total
100
events
$P_t > 0$
40
30
20
10
x
-0.08
-0.04
0
0.04
0.08
N.events
total
200
events
$P_t < 0$
50
40
30
20
10
x
-0.08
-0.04
0
0.04
0.08

FIG. 13

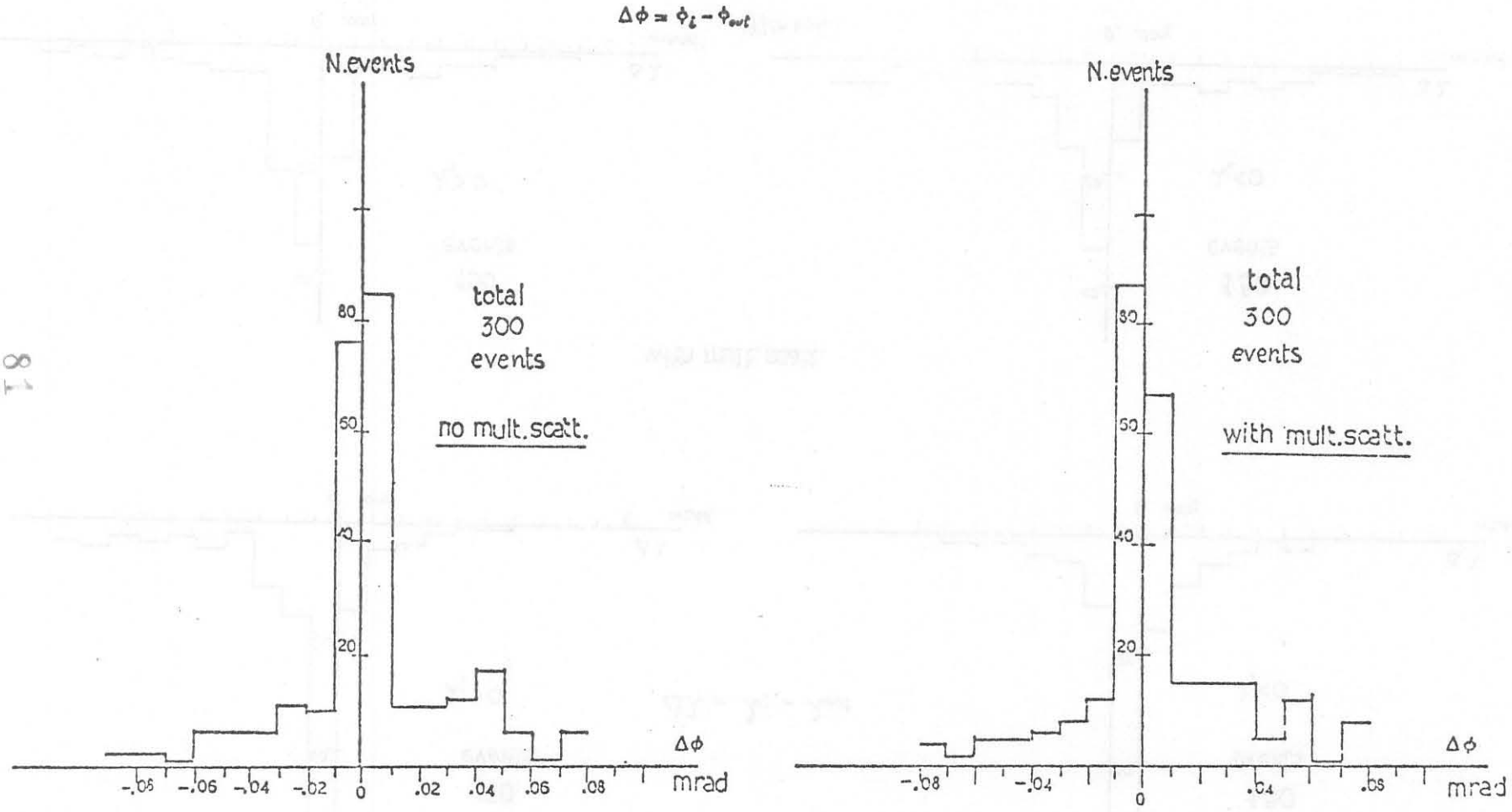
$\Delta\phi = \phi_i - \phi_{out}$
N.events
total
300
events
no mult.scatt.
80
60
40
20
$\Delta\phi$
-.08 -.06 -.04 -.02 0 .02 .04 .06 .08
mrad
N.events
total
300
events
with mult.scatt.
80
60
40
20
$\Delta\phi$
-.08 -.04 0 .04 .08
mrad

FIG. 14

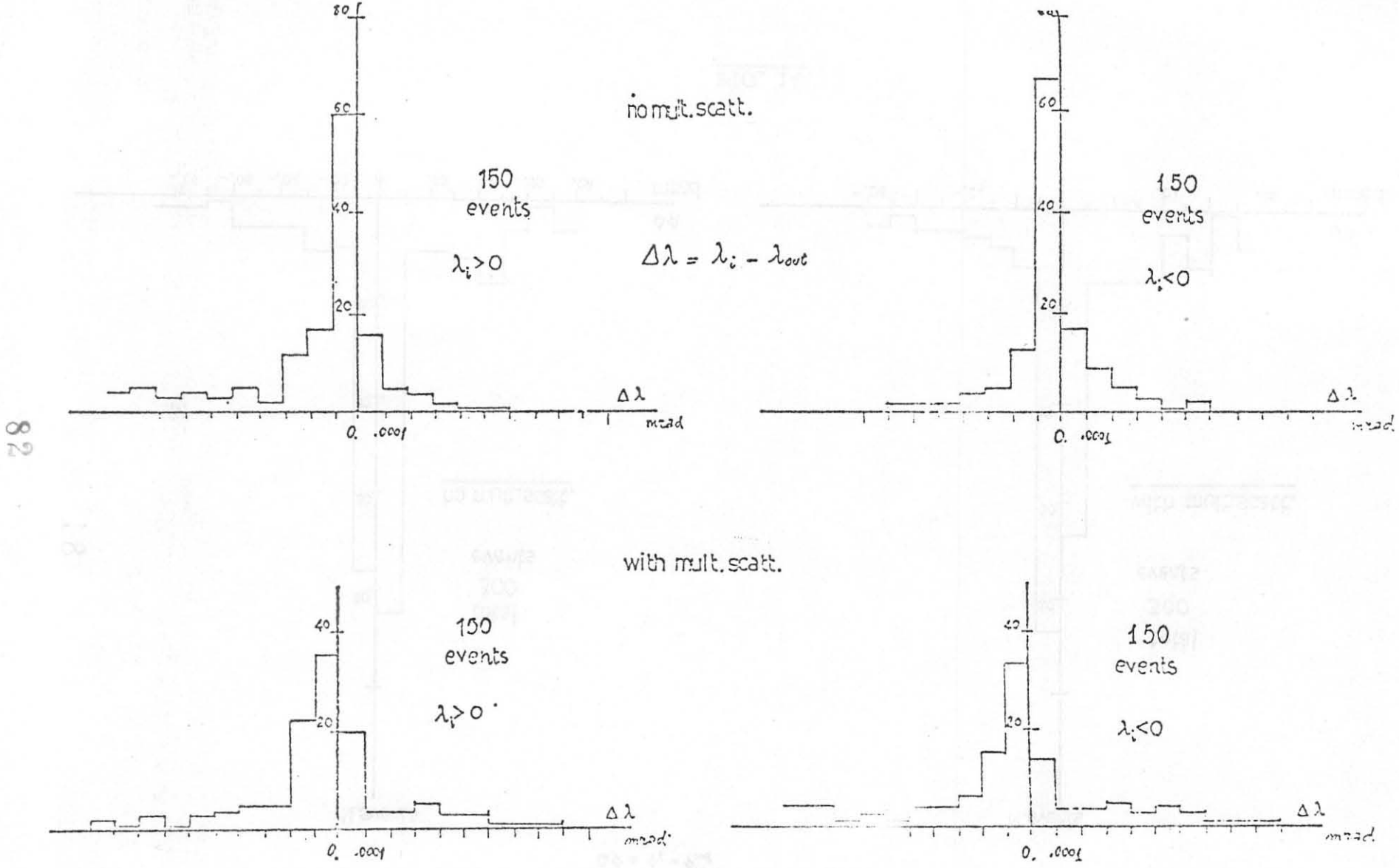
no mult. scatt.
150 events
$\lambda_i > 0$
$\Delta\lambda = \lambda_i - \lambda_{out}$
150 events
$\lambda_i < 0$
with mult. scatt.
150 events
$\lambda_i > 0$
150 events
$\lambda_i < 0$
$\Delta\lambda$
mrad
0. .0001
80
60
40
20

FIG. 15

ACKNOWLEDGEMENTS. -

We wish to thank the Spark Chamber Group of Milan for his collaboration to this work and particularly Prof. G. Vegni, which provided us with many and various informations on the experiment, together with a critical reading of this paper.

REFERENCES. -

(1) - P.Astbury et al., Nuclear Instr. and Meth. 46, 61 (1967).
(2) - P. Muhlemann and J. D. Wilson, High-precision geometrical and kinematical analysis of magnet spark chamber events, CERN 70-17 (1970).
(3) - M. Tarantini, Thesis, Milan University (1974).
(4) - A. Roberts, Intern. Symp. on Nuclear Electronics (Paris, 1963).
(5) - Proposal to study the coherent 3 , 5 and K production on nuclei at the Serpuhhov accelerator, of various authors, PH I/COM--73/32 CERN (1973).